

# RSC Advances



This is an *Accepted Manuscript*, which has been through the Royal Society of Chemistry peer review process and has been accepted for publication.

*Accepted Manuscripts* are published online shortly after acceptance, before technical editing, formatting and proof reading. Using this free service, authors can make their results available to the community, in citable form, before we publish the edited article. This *Accepted Manuscript* will be replaced by the edited, formatted and paginated article as soon as this is available.

You can find more information about *Accepted Manuscripts* in the [Information for Authors](#).

Please note that technical editing may introduce minor changes to the text and/or graphics, which may alter content. The journal's standard [Terms & Conditions](#) and the [Ethical guidelines](#) still apply. In no event shall the Royal Society of Chemistry be held responsible for any errors or omissions in this *Accepted Manuscript* or any consequences arising from the use of any information it contains.



Journal Name

ARTICLE

## A simple strategy to enhance electrical conductivity of nanotubes-conjugate polymer composites via iodine-doping

Received 00th January 20xx,  
Accepted 00th January 20xx

Lina Fan and Xuecheng Xu\*

DOI: 10.1039/x0xx00000x

www.rsc.org/

Iodine-doping is used to develop the high-conductivity carbon nanotube (CNT) -polymer composites. We prepared three kinds of CNT-polymer composites by in-suit polymerization, and obtained iodine-doped samples by mechanical mixing. A series of research about electrical conductivity proves iodine doping is an effective way to get high-conductivity composites with heteroatom in the polymer matrix. The conductivity could increase up to 4 orders of magnitude compared to the undoped samples. Based on Hall-effect, Raman and XPS spectra, we propose the synergistic effect between CNT and iodine results in the superior property. When the heteroatom is N, the synergistic effect of iodine and CNT helps to form stronger p- $\pi$  conjugate system. The N cation radical (as a kind of carriers) increase with the enhanced conjugate, resulting in the improved conductivity. When the heteroatom is S, CNT and iodine form  $\pi$ - $\pi$  conjugate system and charge-transfer complex with S separately. The combination of the two interaction induced the boost of the carrier concentration, as well as the conductivity.

### 1. Introduction

Conductive polymer composites containing insulating polymers and conductive fillers—such as carbon black (CB),<sup>1-3</sup> carbon nanotubes (CNTs)<sup>4-10</sup> and graphene<sup>11-14</sup>—have found wide industrial applications, including in the fields of antistatic materials, self-regulating heaters, over-current, over-temperature protection devices, and electromagnetic interference shielding.<sup>15-19</sup> Among numerous nano-fillers, CNTs are of great interest for its special structure and properties. By this stage, the percolation threshold of the composites could achieve ultralow value.<sup>20-23</sup> However, it is always imperative for the current technical trend to develop advanced CNT composite materials with superior performances, especially for their electrical property.

Iodine-doping, as a kind of classical method to improve the conductivity of polymers,<sup>7, 24-27</sup> is rarely used to get high-conductivity CNT-polymer composites. The very limited works<sup>28-30</sup> did not go deep to research the mechanism systematically, either. To develop the generally applicable method of iodine doping, we prepared CNT-polyaniline (CNT-PANI), CNT-polypyrrole (CNT-PPy) and CNT-polythiophene (CNT-PTh) respectively, explored the conductivity, chemical state and molecular structure. Based on the scientific research, we found only the CNT-polymer composites containing

heteroatoms would have the boosted conductivity after iodine doping. Finally, we obtained the mechanism of synergy, and the mechanism various when the heteroatom differs.

### 2. Experimental

#### 2.1 Materials

CNTs used in this study were supplied by Chengdu Organic Chemicals Co. The CNTs is multi-wall tubes with the 20-30 nm average diameter and the 5-15  $\mu$ m length. Pyrrole, aniline and thiophene monomer were obtained from Sinopharm Chemical Reagent Co. Ammonium persulfate (APS) and hydrochloric acid were also gotten from Sinopharm Chemical Reagent Co. Ethanol and iodine were provided by Shanghai Chemical Reagent Co. and Dongguan united chemical Co. respectively. All the chemicals were used as received without further treatment. Deionized water was used throughout the experiments.

#### 2.2 Preparation of iodine-doped CNT-Polymer composite

The CNT-PPy and CNT-PANI composites were synthesized through in situ polymerization with APS as the oxidizing agent.<sup>31, 32</sup> The CNT and thiophene were in situ polymerized by FeCl<sub>3</sub> in anhydrous chloroform solutions.<sup>33</sup> Then, these CNT-polymer composite powders were blended with iodine by grinding in an agate mortar. After being fully blended, these samples were pressed into wafers with a thickness of about 2 mm and a diameter of about 13 mm at a constant pressure of 20~30 MPa with pressure holding time of 1 min.

#### 2.3 Characterization

The electrical conductivity of the composites was measured by a standard four-probe technique. The carrier concentration and

Department of physics, East China Normal University, No.500 Dong Chuan Road, 200241 Shanghai, China. E-mail: xcxu@phy.ecnu.edu.cn

\*Electronic Supplementary Information (ESI) available: the conductivity of CNTs and CNT-PPA composite after iodine-doping are provided. See DOI: 10.1039/x0xx00000x

carrier mobility were measured by a Hall Effect measurement instrument (HM2000). The measurements are both conducted at room temperature. Raman spectra were carried out by a Jobin-Yvon

**Fig.2** Carrier concentration and mobility ratio of (a) 5%CNT-PANI, (b) 10%CNT-PPy, (c)5%CNT-PTh

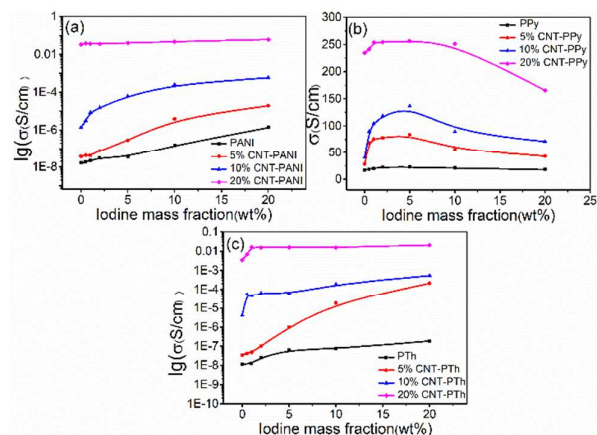


**Fig.1** Conductivities of different CNT-polymer composites with increasing weight fractions of iodine.

LabRAM HR 800 UV spectrometer with a 633 nm line of a He-Ne laser as the exciting source. The surfaces of the composites were analysed by X-ray photoelectron spectroscopy (XPS). The XPS measurements were made on a RBD upgraded PHI-5000C ESCA system (Perkin Elmer).

### 3. Results and discussion

#### 3.1 Electrical characterization subject to different iodine mass fractions

In this study, we have focused on using iodine-doping to obtain high-conductivity composites. Fig.1 (a) is the conductivity of CNT-PANI, while Fig.1 (b) and (c) are the values of CNT-PPy and CNT-PTh. On the one hand, the conductivities of the three kinds of composites are all improved after iodine doping. The conductivity of CNT-PTh increases most sharply (up to 4 orders of magnitude) comparing with the undoped samples, while that of CNT-PANI has a weak growth (about 2 orders of magnitude) and the rise of CNT-PPy is most feeble (only ~3.4 times).

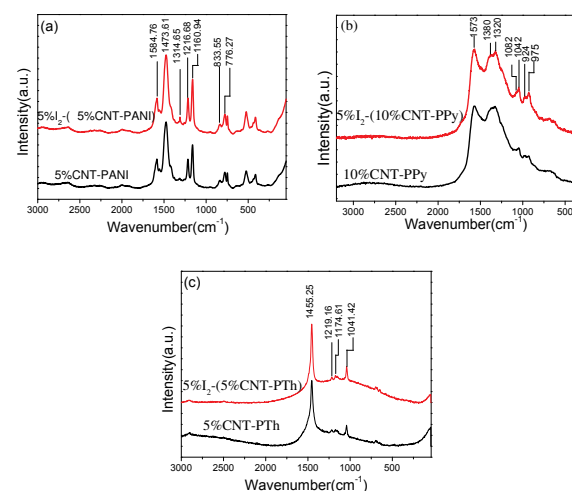
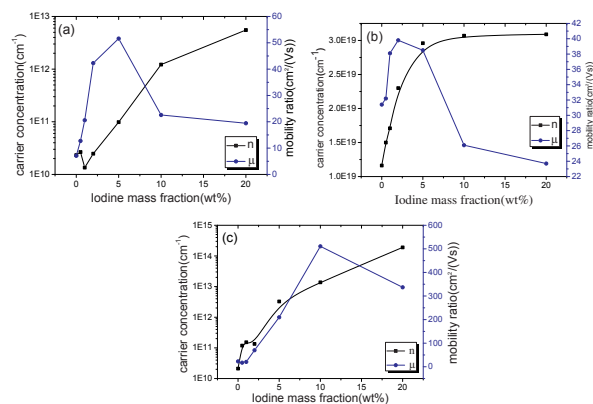


**Fig.3** Raman spectra of the three composites before and after iodine doping

On the other hand, the influences of the components to the conductivity is noticeable. In Fig.1 (a) and (c), the conductivities of pure PANI and PTh have a little growth after iodine doping. When the mass fraction of CNT is 5%, the conductivity of the two composites show a sharp raise with the increasing of iodine. As the CNT content up to 20%, the doped iodine have done little to enhance the conductivity for PANI- and PTh-matrix composites. However, the conductivity of the pure PPy has no obvious change after doping, but that of 10%CNT-PPy raises first and then drops. For the 20%CNT-PPy, the conductivity almost has no increase, only shows the dramatic decrease after iodine doping.

Based on the electrical conductivity equation of semiconductors:  $\sigma = ne\mu$ , where  $\sigma$  is the conductivity,  $e$  is the electron charge,  $n$  and  $\mu$  are the carrier concentration and mobility ratio respectively, we explored the  $n$  and  $\mu$  of the three composites in Fig.2. The carrier concentration of the three composites all grow with the increasing content of the doped iodine. And the mobility ratio show a trend of dropdown after a first rise. The upward tendency of the conductivities are attributed to the carrier concentration and the first raising stage of mobility ratio. At the second period of mobility ratio, the drop tendency of mobility is too weak to influence the conductivity of CNT-PANI and CNT-PTh. But for CNT-PPy, the changes of carrier concentration and mobility are both weak. In this case, the big dip of the mobility ratio results in the decrease of the conductivity.

#### 3.2 Effect of iodine doping on the chemical bonding states

Fig.3 show the Raman spectra of the three composites before and after iodine doping. The curves in Fig.3 (a) contain the most markers for PANI bands. The one located at around  $1584 \text{ cm}^{-1}$  corresponds to carbon-carbon double band stretching vibrations in benzene and quinone rings. The specific bands of C=N stretching modes of imine located at  $1473 \text{ cm}^{-1}$  and C-N stretches of amine

sites at  $1216\text{ cm}^{-1}$ . The stretching vibration of an intermediate bond  $\text{C}\sim\text{N}^+$  is also seen with characteristic frequency around  $1314\text{ cm}^{-1}$ .

Comparing with the undoped samples, the band located at  $1314\text{ cm}^{-1}$  have an obvious

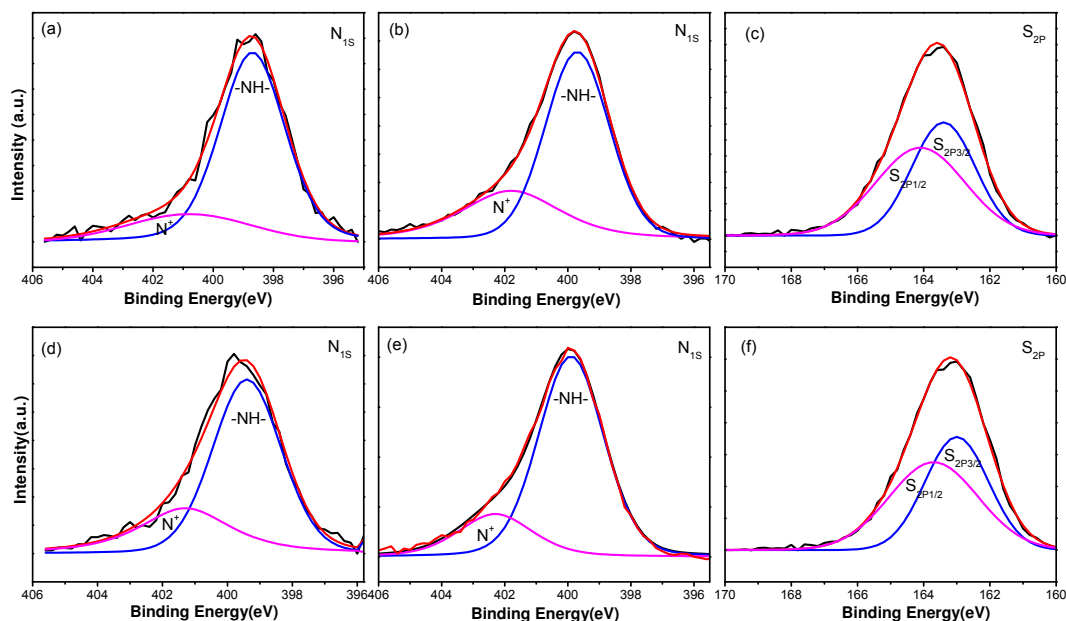


**Fig.4** N1s XPS spectra of (a) undoped and (d) iodine(5%)-doped 5% CNT-PANI; N1s XPS spectra of (b) undoped and (e) iodine(5%)-doped 10% CNT-PPy; S2p XPS spectra of (c) undoped and (f) iodine(5%)-doped 5% CNT-PTh

enhance after iodine doping. Other bands are pretty much the same in CNT-PANI.

In the spectra of CNT-PPy (Fig.3(b)), a strong peak at  $1573\text{ cm}^{-1}$  represents the backbone stretching mode of C-C bonds, and the weak peaks at  $1380$  and  $1320\text{ cm}^{-1}$  are attributed to antisymmetric C-N stretching and the D-band of CNTs, respectively. The peaks at  $935$  and  $1085\text{ cm}^{-1}$  are associated with the bipolaron structure ( $\text{N}^+$ ) and those at  $970$  and  $1060\text{ cm}^{-1}$  associated with the polaron structure ( $\text{N}^{++}$ ).<sup>35</sup> Obviously, the peaks of polaron and bipolaron reinforced after iodine-doping. It indicates the roles of iodine in CNT-PANI and CNT-PPy are both accelerating the generation of nitrogen cation radical ( $\text{N}^+$  and  $\text{N}^{++}$ ).

Different from the former two species, the Raman spectra of CNT-PTh (Fig.3(c)) do not show apparent changes after iodine-doping. This means the effect of iodine in CNT-PTh is different from the other two.

### 3.3 Effect of iodine doping on the chemical states of the heteroatoms

XPS analysis is performed to investigate the chemical states of the heteroatom in CNT-polymer composites (as show in Fig.4). N1s spectra of CNT-PANI and CNT-PPy were deconvoluted into the same set of two components. In Fig.4 (a), the peaks located at  $398.7$  and  $401.1\text{ eV}$  are assigned to the benzenoid amine and nitrogen cationic radical respectively. After iodine-doping (Fig.4 (d)), the two components moved in the direction of high binding energy, located at  $399.2$  and  $400.3\text{ eV}$ . And the percentage of nitrogen cationic radical rose from  $19.9\%$  to  $30.3\%$ . Iodine helps to produced more nitrogen cationic radical.

Similarly, the two components of CNT-PPy have a slightly move, from  $399.6$  and  $401.9\text{ eV}$  to  $400.0$  and  $402.4\text{ eV}$  (Fig. 4 (b) and (e)). The percentage of nitrogen cationic radical went from  $21.0\%$  to  $28.5\%$ . Then, we can get the initial conclusion that iodine play an important role in generating more nitrogen cationic radical when the N heteroatom is existing in the CNT-polymer composites.

The S2p XPS spectra of CNT-PTh are exhibited in Fig. 4(c) and (f). The two components at  $163.3$  and  $164.2\text{ eV}$  is assigned to the neutral

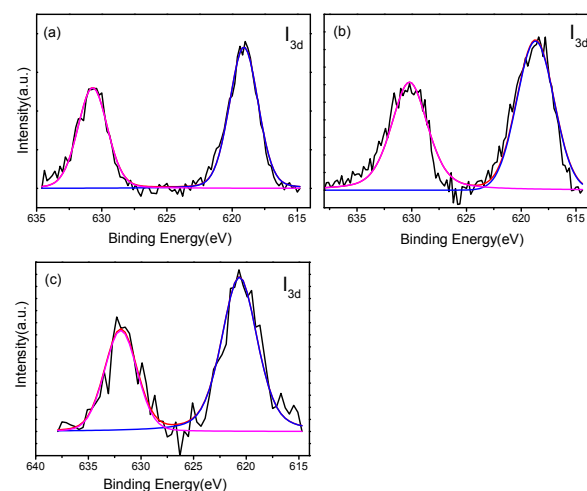


**Fig.5**  $\text{I}_{3d}$  spectra of (a)  $5\% \text{I}_2$ -(5% CNT-PANI); (b)  $5\% \text{I}_2$ -(10% CNT-PPy) and (c)  $5\% \text{I}_2$ -(5% CNT-PTh)

S 2p<sub>3/2</sub>, and the oxidized S 2p<sub>1/2</sub>. Different from the former two composites, we did not find the positively charged sulfur (S<sup>δ+</sup>) at about 167.5eV after iodine doping.<sup>36</sup> The two components shifted slightly to the low binding energy direction, located at 162.9 and 163.6 eV finally. This further demonstrates the effect of iodine in CNT-PTh is different from the other two composites. To further explore the function of iodine, the I3d XPS spectra are shown in Fig.5. The two peaks of the standard iodine spectra located at 619.5 and 631.0 eV. When doped into the three composites, the peaks display various degrees of movement. For I<sub>2</sub>-CNT-PANI, the two peaks located at 619.0(-0.5 eV relative shift) and 630.6 eV (-0.4 eV relative shift). The changes of the spectrum of I<sub>2</sub>-CNT-PPy is similar with the previous one. The two peaks move from 619.5 and 631.0eV

to 618.7 and 630.2eV, have -0.8 eV relative shift respectively. In Fig.5 (c), the peaks moved to the higher direction of the binding energy and centered at 620.7 and 632.0 eV finally. This means the electron density around iodine in CNT-PANI and CNT-PPy increased, but in CNT-PTh decreased.

### 3.4 Mechanism

In our former research, we doped CNTs (ESI Figure S1), conjugated polymers and CNT-polymer composites with iodine respectively. We find the conductivity of pure CNTs have a little decrease after iodine doping, and that of pure polymers have slightly increase except PANI. For PANI, the protonation effect lead to the rising of the conductivity. Only the conductivity of iodine doped CNT-polymer composite sharply grow compared with undoped sample. On this basis, we proposed the synergistic effect between iodine and CNT lead to the increase of the conductivity.

To move a further step, we collected several CNT-conjugated polymer composites to research the iodine-doping effect. Surprisingly, only the CNT-polymer composites contain heteroatom in the polymer matrix show a boost conductivity after iodine-doping. The other composites, like CNT-PPA (ESI Figure S2), even show a decrease conductivity after doping. Based on these facts, we believed the synergy of CNT and iodine functions on the heteroatom in polymer matrix. In addition, we found the mechanisms of action dissimilar when the heteroatom was different.

For CNT-PANI and CNT-PPy, they both contain nitrogen atoms, the synergistic effect helps to generate more carrier. The process is as follows: after iodine-doping, there would be a p-π conjugation system between the doped iodine and CNT-polymer. This system is surely much stronger than that in iodine-doped polymer because of the synergy of CNT and iodine. The enlarged conjugation make the lone electron pair of N delocalized to a larger range, which promote to generate more nitrogen cationic radical. These increased cationic radical, as evidenced from Raman and N1s XPS spectra, provides more carrier in the doped composites, leading to stronger conductive ability (shown in Fig.1 and 2). The increase conjugate degree of the composites improves the mobility ratio at the same time. With increasing iodine-doping concentration, the impact of neutral impurity scattering becomes more significant. It will adversely reduce the mobility ratio in this case. As a result, the conductivity of iodine-doped CNT-PPy exhibits a drop down trend.

But for CNT-PANI, the influence of mobility ratio is much smaller than carrier concentration, the conductivity doesn't have a decrease.

However, the synergistic effect is totally different as the heteroatom is S. For CNT-PTh, there is a π-π conjugation between CNT and PTh. Only one lone pair electron of S could involve in the conjugation system because of the directivity of electron pair. After iodine doping, the other lone pair of electrons of S will shifted to iodine for the stronger electronegativity of iodine. This means the composites and iodine form a charge-transfer complex<sup>37</sup> besides the π-π conjugation system. As a result, the peaks of S2p move in the direction of higher binding energy and peaks of I3d in the opposite direction. With the synergistic effect of so-called charge-transfer complex and π-π conjugation system, the concentration of carriers boosted, and the conductivity of the materials shoot up. But for iodine doped PTh, there is only one kinds of interaction to improve the carrier concentration. That's why the conductivity of iodine doped PTh do not have such sharply increase. With the increasing content of iodine, the excess iodine lowers the mobility ratio in return. The conductivity did not show obvious decrease, because the influence of mobility ratio is really little compared with the carrier concentration.

### 3. Conclusions

In conclusion, we successfully demonstrated that it is effective to obtain highly conductive CNT-polymer composites via an iodine-doping process. And only the composites containing heteroatom in the polymer matrix have an increasing conductivity after iodine doping. The conductivity of such doped composites could raise up to 4 orders of magnitude of the undoped samples. The mechanism is diverse if the heteroatom differs. When the heteroatom is N, the conductive increased process is a nitrogen cationic radical-growth process. Based on the synergistic effect of iodine and CNT, the p-π conjugation enhanced and produced more nitrogen cationic radical. Differently, in the polymer-matrix composites containing S atom, there is charge-transfer complex and conjugate system at the same time. Under the influence of the two interaction, the carrier concentration, as well as the conductivity grow. With the mechanism being explored, iodine doping is valid to get a class of high-conductivity polymer composites besides CNT-PANI, CNT-PPy and CNT-PTh. It is significant to develop both the advance materials and the iodine-doping theory.

### Notes and references

- 1 T. M. TAWALBEH, S. SAQAN, S. F. YASIN1, A. M. ZIHLIF, G. RAGOSTA, *J. Mater. Sci.*, 2005, **16**, 351-354.
- 2 H. Horibe, T. Kamimura and K. Yoshida, *J. Appl. Phys.*, 2005, **44**, 2025-2029.
- 3 F. El-Tantawy, K. Kamada and H. Ohnabe, *Mater. Lett.*, 2002, **56**, 112-126.
- 4 M. F. De Volder, S. H. Tawfik, R. H. Baughman and A. J. Hart, *Science*, 2013, **339**, 535-539.
- 5 E. Murugan and V. Gopi, *J. Phys. Chem. C*, 2011, **115**, 19897-19909.
- 6 W. Li, Y. Zhang, J. Yang, J. Zhang, Y. Niu and Z. Wang, *ACS Appl. Mater. Interfaces*, 2012, **4**, 6468-6478.
- 7 A. B. Kaiser, *Rep. Prog. Phys.*, 2000, **64**, 1-49.

- 8 T. W. Lee and Y. G. Jeong, *Compos. Sci. Technol.*, 2014, **103**, 78-84.
- 9 H. Pang, D. X. Yan, Y. Bao, J. B. Chen, C. Chen and Z. M. Li, *J. Mater. Chem.*, 2012, **22**, 23568-23575.
- 10 W. Guo, C. Liu, X. Sun, Z. Yang, H. G. Kia and H. Peng, *J. Mater. Chem.*, 2012, **22**, 903-908.
- 11 M. Shtein, R. Nadiv, M. Buzaglo, K. Kahil and O. Regev, *Chem. Mater.*, 2015, **27**, 2100-2106.
- 12 J. Syurik, O. A. Ageev, D. I. Cherednichenko, B. G. Konoplev and A. Alexeev, *Carbon*, 2013, **63**, 317-323.
- 13 F. Hu, W. Li, J. Zhang and W. Meng, *J. Mater. Sci. Technol.*, 2014, **30**, 321-327.
- 14 L. Ma, H. Niu, J. Cai, P. Zhao, C. Wang, Y. Lian, X. Bai and W. Wang, *J. Mater. Chem. C*, 2014, **2**, 2272-2282.
- 15 P. Barpanda, K. Djellab, R. K. Sadangi, A. K. Sahu, D. Roy and K. Sun, *Carbon*, 2010, **48**, 4178-4189.
- 16 G. A. Gelves, M. H. Al-Saleh and U. Sundararaj, *J. Mater. Chem.*, 2011, **21**, 829-836.
- 17 T. Zhou, J. W. Zha, Y. Hou, D. Wang, J. Zhao and Z.-M. Dang, *ACS Appl. Mater. Interfaces*, 2011, **3**, 4557-4560.
- 18 S. M. R. Bera, B. B. Khatua, *J. Appl. Polym. Sci.*, 2015, **42161**, 1-10.
- 19 C. Yang, C. P. Wong and M. M. F. Yuen, *J. Mater. Chem. C*, 2013, **1**, 4052-4069.
- 20 W. Bauhofer and J. Z. Kovacs, *Compos. Sci. Technol.*, 2009, **69**, 1486-1498.
- 21 E. Bilotti, H. Zhang, H. Deng, R. Zhang, Q. Fu and T. Peijs, *Compos. Sci. Technol.*, 2013, **74**, 85-90.
- 22 X. Zhang, X. Yan, Q. He, H. Wei, J. Long, J. Guo, H. Gu, J. Yu, J. Liu, D. Ding, L. Sun, S. Wei and Z. Guo, *ACS Appl. Mater. Interfaces*, 2015, **7**, 6125-6138.
- 23 A. V. Kyrlyuk and P. Schoot, *PNAS*, 2008, **105**, 8221-8226.
- 24 Z. X. Rong and K. T. Man, *J. Polym. Sci. B*, 1997, **35**, 1993-2001.
- 25 M. Hishinuma and T. Yamamoto, *J. Mater. Sci. Lett.*, 1984, **3**, 799-801.
- 26 S. Moulay, *J. Polym. Eng.*, 2013, **33**, 389-443.
- 27 C. K. Chiang, Y. W. Park, A. J. Heeger, H. Shirakawa, E. J. Louis and A. G. MacDiarmid, *J. Chem. Phys.*, 1978, **69**, 5098.
- 28 Y. Bin, Q. Chen, K. Tashiro and M. Matsuo, *Phys. Rev. B*, 2008, **77**, 035419(1-7).
- 29 B. R. Sankapal, K. Setyowati, C. Jian and L. Haiying, *Applied Physics Letters*, 2007, **91**, 173103(1-3).
- 30 P. Jha, S. P. Koiry, V. Saxena, P. Veerender, A. K. Chauhan, D. K. Aswal and S. K. Gupta, *Macromolecules*, 2011, **44**, 4583-4585.
- 31 B. Yu and X. Xu, *RSC Adv.*, 2014, **4**, 3966-3973.
- 32 L. Li, Z. Y. Qin, X. Liang, Q. Q. Fan, Y. Q. Lu, W. H. Wu, and M. F. Zhu, *J. Phys. Chem. C*, 2009, **113**, 5502-5507.
- 33 L. Wang, X. Jia, D. Wang, G. Zhu and J. Li, *Synth. Met.*, 2013, **181**, 79-85.
- 34 H. S. Abdullah, *Int. J. Phys. Sci.*, 2012, **7**, 5468-5476.
- 35 Y. W. Lin and T. M. Wu, *Polym. Int.* 2010, **60**, 382-388.
- 36 H. C. Liang and X. Z. Li, *Appl. Catal. B*, 2009, **86**, 8-17.
- 37 S. K. Singh, R. K. Gupta and R. A. Singh, *Synth. Met.*, 2009, **159**, 2478-2485.